Enhancing vibration measurements by Mössbauer effect

G. A. Pasquevich, A. Veiga, P. Mendoza Zélis, N. Martínez, M. Fernández van Raap & F. H. Sánchez

Hyperfine Interactions

ISSN 0304-3843
Volume 224
Combined 1-3

Hyperfine Interact (2014) 224:205-215
DOI 10.1007/s10751-013-0844-3

Springer

Hyperfine Interact (2014) 224:205–215
DOI 10.1007/s10751-013-0844-3

Enhancing vibration measurements by Mössbauer effect

G. A. Pasquevich · A. Veiga · P. Mendoza Zélis · N. Martínez · M. Fernández van Raap · F. H. Sánchez

Published online: 13 March 2013

Abstract The measurement of the Mössbauer effect in a system excited with a periodic perturbation can provide information about it. For that purpose, the Mössbauer absorption of a source-absorber set which hyperfine parameters are well known, is measured at a constant relative velocity (i.e. at a defined spectral energy). The resulting Mössbauer absorption periodic signal provides information of the sample *ac* perturbation response. This approach has been used time ago to measure small tympanic vibrations (mechanical perturbations). In this work we present an extension of the vibration experiments, by measuring them at various absorber-source relative velocities within a constant-velocity strategy. As a demonstration test, the frequency response of a piezoelectric diaphragm in the 100 Hz–5 kHz range is obtained with a custom electronic counter. The experiments are performed using a ^{57}Co(*Rh*) source and a 25-μm-thick stainless-steel absorber fixed to a piezoelectric diaphragm. Phase shifts and amplitude vibrations with velocities in the range from 1.5 μm/s to 20 mm/s are well characterized, extending the linearity limit well beyond the earlier suggested one of 1 mm/s.

Keywords Vibrations · Mössbauer · Velocity

Proceedings of the thirteenth Latin American Conference on the Applications of the Mössbauer Effect, (LACAME 2012), Medellín, Columbia, 11–16 November 2012.

G. A. Pasquevich (✉) · A. Veiga
Facultad de Ingeniería, UNLP, La Plata, Argentina
e-mail: gpasquev@fisica.unlp.edu.ar

G. A. Pasquevich · A. Veiga · P. Mendoza Zélis · M. Fernández van Raap · F. H. Sánchez
Instituto de Física La Plata, CONICET, La Plata, Argentina

N. Martínez · P. Mendoza Zélis · M. Fernández van Raap · F. H. Sánchez
Facultad de Ciencias Exactas, UNLP, La Plata, Argentina

N. Martínez
CICpBA, La Plata, Argentina

1 Introduction

The measurement of Mössbauer effect synchronously with a periodic excitation at a defined constant Doppler energy can be used to obtain the dynamic response of a perturbed sample. Variations on the intensity, position, or other parameters of the Mössabuer spectral lines can be interpreted as a characterization of the perturbation and its effect on the sample.

Relative movements induced by an external perturbation can be detected by Mössbauer effect. In fact, Mössbauer spectroscopy is based on relative motion through Doppler Effect: a Mössbauer spectrum display absorption versus relative velocity. Therefore, if the spectrum is well known, changes in the absorption can be interpreted as a measurement of the relative velocity.

This approach has been widely used to characterize basilar-membrane frequency responses of different species [1–6]. The pioneering work in this line is from 1967 by P. Gilad et al. [1] in which a single line absorbent and a counter synchronized with a sound generator is used to study the tympanic membrane response of guinea pigs in the range from 250 Hz to 9 kHz. All those works have been of major importance in its discipline, they are still relevant and are being cited up to day.

In addition to biologic applications, mechanical vibration studied by Mössbauer effect has some characteristics that makes it powerful and unique. Hence should not be let aside. Accordingly, we can mention: the ability of the gamma ray to pass through opaque materials, and the atomic selectivity of the Mössbauer effect. The former allows the study of internal parts in macroscopic complex systems such as instruments, machines, etc.; the latter (the ability to distinguish different structural phases of the same atom) let the study of particular locations into micro-scale complex systems (e.g. soft condensed matter materials).

The procedure used to detect and quantify effects of vibrations by Mössbauer effect consists on measuring the Mössbauer absorption synchronously with the vibration source at a chosen position (velocity) in the spectrum. It means that the source-absorber relative velocity has a steady (*dc*) component, to adjust that point (constant velocity) and a superimposed harmonic wave (*ac*) producing the perturbation. The sensitivity of the method depends strongly on the constant velocity selection. For low amplitude perturbations, the most sensitivity spectral position corresponds to the one of maximal slope. Relative movements induced in the absorbent appear as changes in the relative velocity that produce variations in the transmission rate which are proportional to the spectrum slope. Note that in all the previous works (related to tympanic response) the radiation source was attached rigidly to the membrane to be characterized and the absorber was at rest in the laboratory frame. Therefore, the *dc* constant velocity was zero. This velocity election is the simplest way to perform this kind of experiments, since no electronic velocity branch is needed. In those cases, the slope at the zero velocity spectral position is just determined by the relative isomer shifts of the source and absorber. In what follows, we will assume a geometry in which the absorber is fixed to the sample (which will be perturbed) while the radioactive source is used to select the constant velocity relative to the laboratory frame. Although both geometries are equivalent, the latter is the one used in the experiments of this work.

Let us assume a sinusoidal time perturbation ε of frequency f and amplitude ε_0,

$$\varepsilon(t) = \varepsilon_0 \sin(2\pi f t) \tag{1}$$

under which the absorber oscillates. Let us also assume a linear absorber movement response, in such a way that the response of the absorber-velocity V is only defined by an amplitude V_0 and a phase-shift φ,

$$V(t) = V_0 \sin(2\pi f t + \varphi) \tag{2}$$

If the source is moved at a constant velocity v, corresponding to a flank of a spectral absorption line, and if the resulting V_0 is low enough, then the transmission rate r will harmonically oscillate retaining information about the amplitude and phase-shift of the velocity response:

$$r(t) = r_0 + \alpha V_0 \sin(2\pi f t + \varphi), \tag{3}$$

where r_0 is the rate in absence of perturbation and α is the spectrum slope $(\partial r/\partial v)$ at the constant velocity position. For higher amplitudes the shape of the absorption line introduces non linearities and the last equation is not valid any more. This nonlinearity puts a limit to the maximum amplitudes than can be retrieved through this methodology. This limit was estimated around 1 mm/s, a rough evaluation of the effective velocity wideness of an absorption line [4, 7].

The Mössbauer characterization of vibrations at different constant velocities improves considerably the limitations previously mentioned. Besides, the ability of measuring synchronized Mössbauer signals allows the incursion in other kind of perturbation studies as the recently proposed magnetic susceptibility study by Mössabuer effect [8], which is a frequency extension of the Mössbauer magnetic scans [9]. Therefore, the development of equipments with this facilities is of interest. In this work we present a complete device with the ability of performing synchronous Mössbauer experiments. The test of the equipment is carried out characterizing a commercial piezoelectric diaphragm, by studying oscillations up to 5 kHz induced on a rigidly attached stainless steel sheet.

2 Experimental details

A piezoelectric diaphragm (PD) 7BB-35-3 from muRata Manufacturing was used for the experimental set-up. A 5 mm hole was perforated in its center to act as a window for the gamma ray. A 25 μm thick stainless-steel sheet (the absorber), mounted between two acrylic plates of 1 mm thick, was fixed to the PD covering the hole. The PD was fed with an harmonic *ac* signal generated by a driver as is shown in the Fig. 1. The stainless steel foil was carefully fasten to assure its motion represents the PD motion.

A multichannel scaler (MCS) designed in our laboratory [10] was used as wave reference generator for the PD excitation and as a multiscaler for the data acquisition. With this custom equipment, frequencies up to 75 kHz can be reached when only four acquisition channels are used. The constant velocity module (CVM), also designed in our laboratory [11], generates a rectangular asymmetric wave with zero mean value as a velocity reference wave for the velocity drive. The generated wave was carefully designed, considering the driver and transducer transfer function, in order to achieve a high quality constant velocity state as well a good temporal efficiency [11]. A logic signal synchronized with the velocity wave was also generated to enable the MCS to count only at the constant part of the velocity wave.

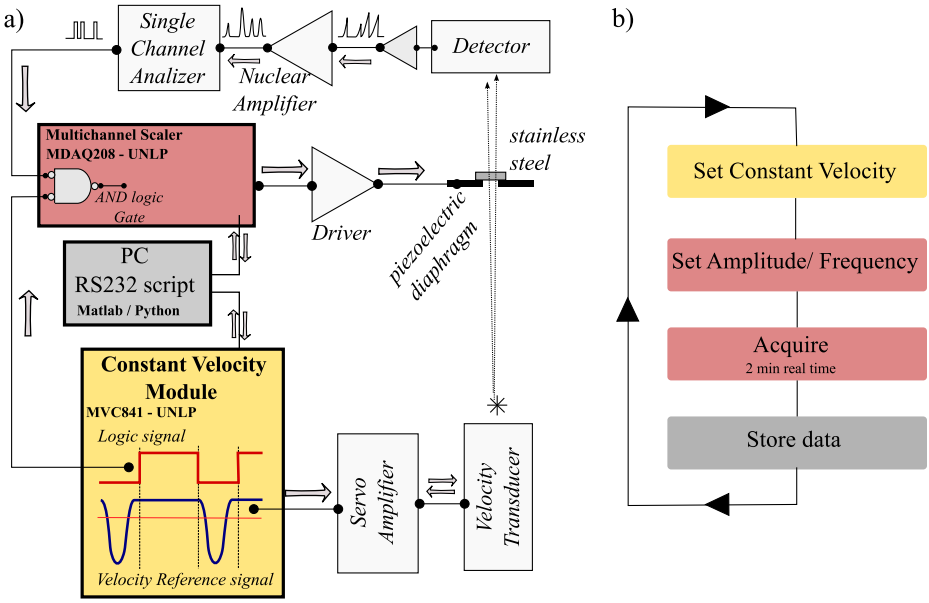

Fig. 1 **a** Experimental layout used to count 14.4 keV events in a synchronous way with a harmonic perturbation. The synchronous counting is carried out while the source is moved at constant velocity relative to the laboratory frame. **b** Flow diagram of the protocol used to measure different perturbation frequencies and amplitudes as well as different velocities during experiments

Both modules are connected to a personal computer using an RS232 serial protocol. Amplitude and frequency of the excitation wave are managed externally through the RS232 protocol. A Python 2.6 script on the computer was used to simultaneously drive both modules. A flow diagram of the script is shown at Fig. 1b.

The velocity calibration was performed by full spectra acquisition of three different calibration samples: alpha iron, stainless-steel and bulk magnetite. All the velocities given in this work are given relative to the Laboratory Frame, i.e. they are referenced to isomer shift of ^{57}Fe(Rh).

Two kinds of experiments were performed: frequency characterization of the piezoelectric response in the range 100 Hz to 5 kHz, and amplitude response at a fixed frequency (near resonance).

3 Frequency domain

For frequency characterization of the piezoelectric response, three velocities values were selected. Two at the highest slope values of the left and right flanks of the absorption lines (−0.49 and 0.03 mm/s respectively). The third at −3.52 mm/s, where resonant absorption in absence of perturbation is zero, i.e background velocity. The position are shown with vertical arrows in Fig. 2.

The range from 100 Hz to 4.4 kHz was sampled at two different PD voltage amplitudes: 90 mV and 150 mV. The corresponding results are shown in Fig. 3a and

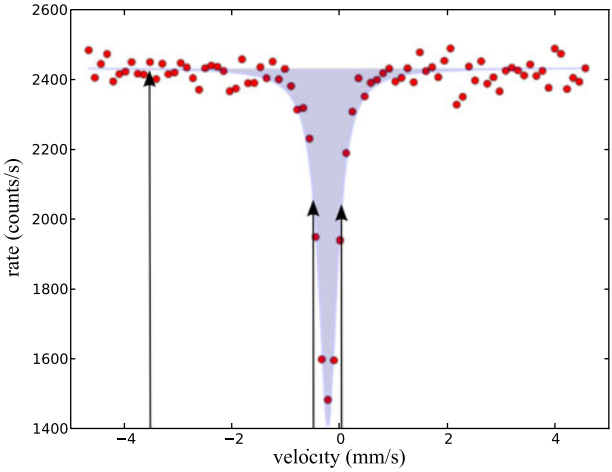

Fig. 2 Stainless-steel Mössbauer spectrum. Fixed velocities (−3.52 mm/s, −0,49 mm/s and 0.03 mm/s) chosen to perform the frequency characterization are indicated with *arrows*. The velocities are expressed relative to ^{57}Fe(*Rh*) isomer shift (i.e. to the laboratory frame)

b respectively. In each graph transmission vs. phase ($2\pi t/T$) of each of the three velocities are plotted. The L and R curves correspond to left and right flanks velocity positions (−0.49 and 0.03 mm/s respectively) while the B curve corresponds to the high velocity position (background).

At low and high frequencies transmission rate oscillations are harmonic enough as to follow (3). For frequencies between 2 kHz and 3 kHz, around resonance, the transmission response becomes nonlinear and it can be seen as a double peak response. The figure also shows a relative phase shift of 180° for all frequencies between R and L curves. It is apparent since the curves represent the behavior at each side of the absorption line. For the higher amplitudes near 2.4 kHz the transit of the whole absorption line can be appreciated over both flanks positions. This manifestations are more evident in the experiment at higher voltage amplitude (Fig. 3b).

In order to retrieve information on the amplitude V_0 and phase-shift φ from the data, the temporal transmission rate dependence was modeled as the absorption of a Lorentzian line whose center oscillates sinusoidally,

$$r(t; v_i, V_0, \varphi) = 1 - \frac{\Gamma^2}{4} \frac{h}{(\delta_0 - v_i - V_0 \sin(2\pi f t + \varphi))^2 + \frac{\Gamma^2}{4}} \tag{4}$$

where δ_0 and Γ are the isomeric shift and linewidth, h is the line depth, v_i with $i = 1, 2, 3$ are the three constant velocities. A multiple fit at the selected velocities was performed over all the frequencies range. Γ, h and δ_0 were common parameters to all the velocities and frequencies. V_0 and φ parameters were different for each frequency, but common for the three velocities. The three v_i were fixed parameters. The resulting fitted curve for each velocity is shown in Fig. 3 (solid black curve). Note that the explicit Lorentzian shape in the model incorporates the nonlinearity of the absorption profile to the analysis. On the other hand the explicit harmonic temporal dependence of the line center restricts the model to situations in which the PD responds linearly to the *ac* input voltage.

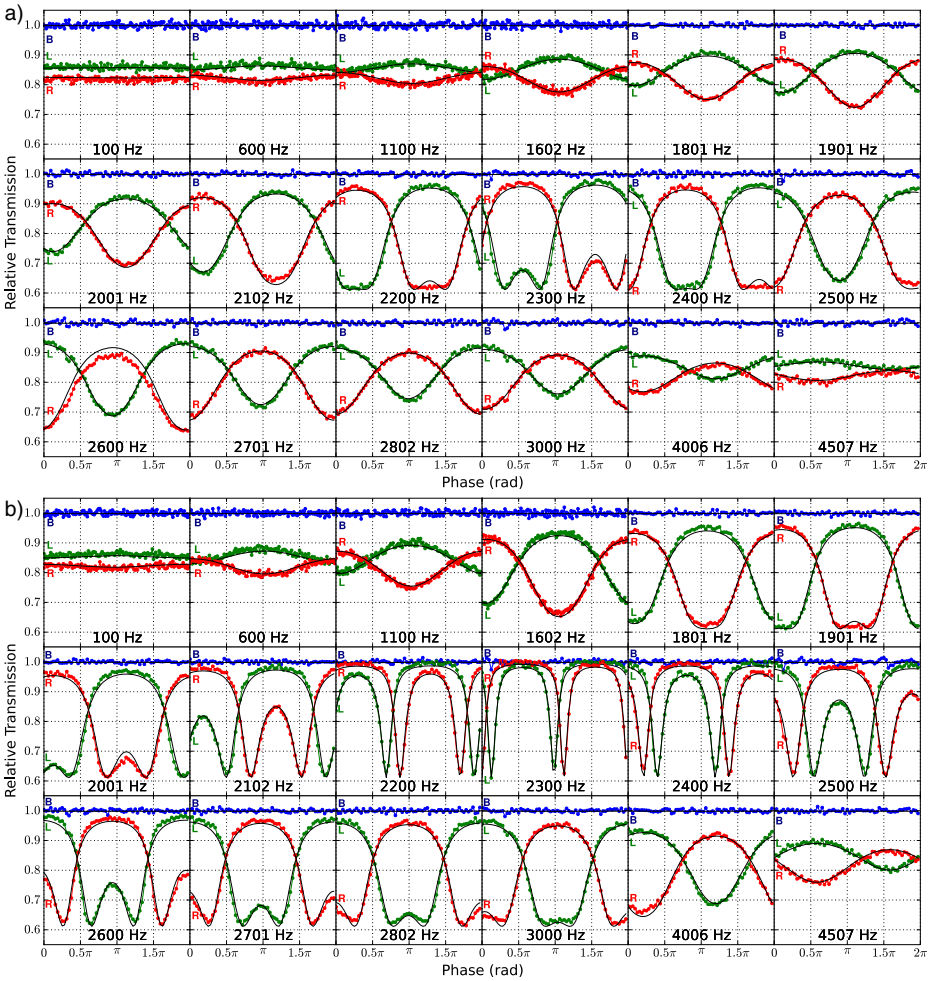

Fig. 3 Transmission rate at the three velocities indicated in Fig. 2. The curves indicated by R, L and B correspond to the fixed velocities at −3.52, −0.49 and 0.03 mm/s. They are related to the left and right flank of the absorption line and a background position, respectively. **a** Transmission response to 90 mV *ac* input voltage. **b** Response to 150 mV *ac* input voltage

From the fit procedure, amplitude and phase-shift of the PD response were determined in the whole frequency range (Fig. 4a and b). A resonance peak is observed at 2.3 kHz for both perturbation amplitudes. At this frequency a $\pi/2$ phase-shift change respect to low frequencies value is achieved, and completes to a net relative change π as the frequency increases. Moreover, a further change in curve's slopes can be noted at a frequency around 4 kHz. In terms of pole-zero diagrams this behavior corresponds to a linear third order system with a zero at the origin. The change in the PD input amplitude was reflected only as an increase in the velocity amplitude. The phase-shift was not affected by this parameter.

The above experiment is a good example of a system characterization using the method proposed in the present work.

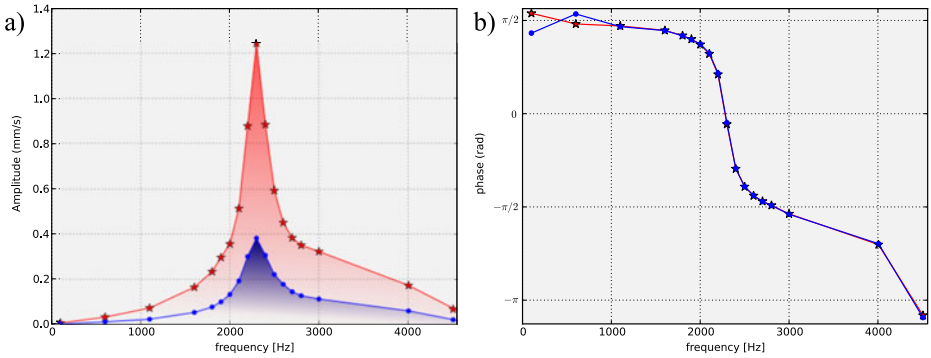

Fig. 4 Results of the multiple fit: **a** amplitude and **b** phase-shift as a function of the frequency for each PD ac-voltage amplitude (90 mV: *blue dots*, 150 mV: *red stars*)

On this set of experiments the extreme velocity amplitudes were 1.5 μm/s ($f = 100$ Hz, $\varepsilon_0 = 90$ mV) and 1.24 mm/s ($f = 2.3$ kHz, $\varepsilon_0 = 150$ mV). Since the movement is harmonic, the position amplitude can be deduced through $\Delta x = \frac{\Delta v}{2\pi f}$. The smallest position amplitude was 0.7 nm ($f = 4.5$ kHz, $\varepsilon_0 = 90$ mV) and the highest was 85 μm at ($f = 2.3$ kHz, $\varepsilon_0 = 150$ mV).

4 Amplitude domain

In order to characterize high amplitude vibrations, a large number of velocities covering a wider range is needed. A uniformly distributed set of twenty one velocities was chosen to characterize vibrations in the range from −10 mm/s to 10 mm/s. The transmission at each constant velocity was recorded at four voltage amplitudes of 1, 2, 4 and 8 V. The experiments were carried out at 2.4 kHz; a near resonance frequency selected to achieve high amplitudes with the available voltages. The phase was sampled in $N_{CH} = 64$ uniformly distributed channels.

The measured transmission as a function of phase and velocity is shown as 2D contour graphs in Fig. 5a. The Mössbauer transmission defines a surface in the *phase-velocity* space. The transmission at each point of this space is given by the color scale at the right side of the contour-graphs: light colors correspond to high transmission and dark colors to low transmission.

The velocity trace of the transmission surface at the velocity −0.2 mm/s is shown in Fig. 5b. This velocity corresponds to the center of the absorption line in absence of perturbation (i.e. the stainless-steel isomer shift). It is marked over the contour graphs with a dotted horizontal line. These traces show the two instants at which the absorption-line center coincides with −0.2 m/s, i.e. the moments at which the absorber is at rest relative to the laboratory. Note that these traces are equivalent to the plots shown in Fig. 3. Similarly, 0.15 rad phase traces are plotted in Fig. 5c. Again, the 0.15 rad phase is marked as a dotted vertical line on the contour graphs. This phase corresponds to one of the instant at which the absorber passes through its rest point.

To quantify φ and V_0 for each case a multiple fit of each data set was performed using (4). The velocity center of the absorption line, according to the resulting fitted

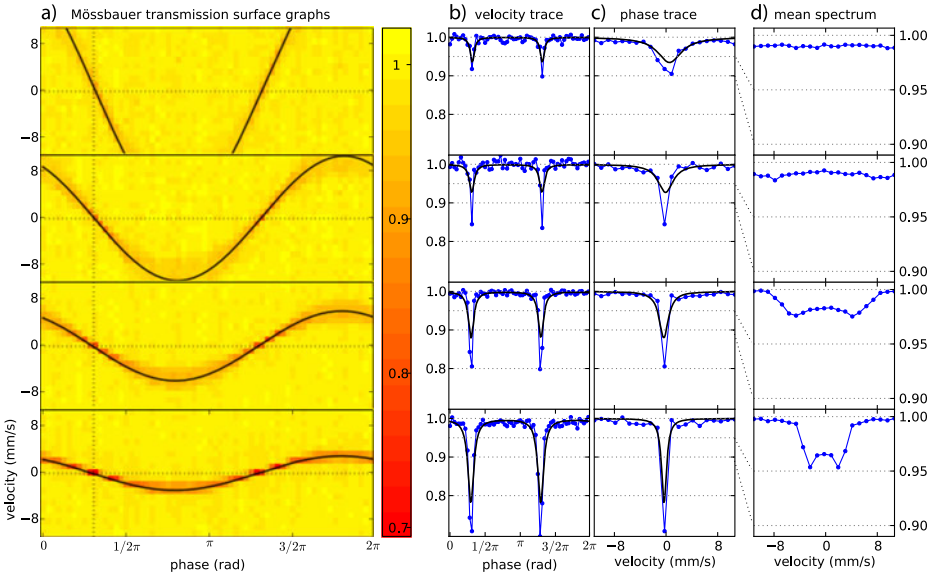

Fig. 5 **a** Contour graphs of Mössbauer transmission surface as a function of phase (abscissa) and constant velocity (ordinate). From bottom to top each graph corresponds to 1, 2, 4 and 8 V amplitude of the ac PD voltage input. The transmission intensity is given by right color scale. The *solid black line* indicates the center of the absorption line according to the least-square-fit result. **b** Velocity trace of the transmission surface at the velocity −0.2 mm/s (indicated as a *horizontal dotted line* in the contour graph). The *solid black line* is the velocity trace of the fitted surface. **c** Phase trace at 0.15 rad (indicated in the contour graph as a *vertical dotted line*). The *solid black line* is the surface trace. **d** Mean Mössbauer spectrum: average on phase of the transmission surface

surface, is plotted vs. phase over the contour graphs (solid black curve). In the same way, the fitted-surface velocity and phase traces are compared with the experimental traces in the corresponding axes.

From the fit procedure it is deduced that the phase shift ($\varphi = -0.8\pi$) remains quite independent of the input voltage amplitude. This conclusion was easily anticipated by a raw inspection of the contour graphs. The velocity amplitude displayed a linear dependence on the voltage amplitude. The amplitudes obtained from this fit analysis, together with the ones obtained in the previous section (for 2.4 kHz), are plotted in Fig. 6 evidencing the mentioned linearity. The maximum sensed amplitude is 20.6 mm/s.

Some cautionary remarks about experimental and fitting results shown in Fig. 5. First, when the line is passing near −0.2 mm/s (i.e. the rest point) the depth of the absorption-line decreases as V_0 increases (see Fig. 5a, b and c). This is an average effect related to the finite acquisition time of each MCS-channel (dwell-time t_d) and the movement of the absorption line. The quickest the absorption line moves through a constant velocity value, the lesser the time it will be contributing to the measured transmission of the corresponding channel. In other words, if the absorber velocity changes during t_d an amount ΔV of the order or larger than the line halfwidth, the recorded transmission at the channel will be related to the absorption time average of the moving line. As a consequence, the measured depth of the absorption line seems to be lower than the real one. In such cases, the time fraction that the line

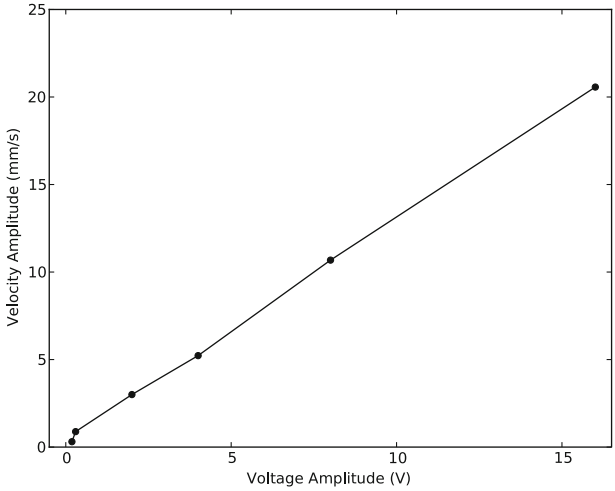

Fig. 6 Velocity amplitude vs. PD voltage amplitude obtained from fit analysis shown in Figs. 3 and 5

is not contributing to this velocity channel, it will be doing so at the neighboring channels. Hence, this line movement is also manifested as an increase of the observed linewidth in constant phase traces (Fig. 5c). Note that since it is an effect related with the instantaneous velocity change of the absorber, it will be more evident when the line moves faster, which occurs around the rest point zones.

Do not confuse this quick movement effect with the vibration effect over a Mössbauer spectrum. Although both consequences are related to vibrations, the technical origin is different as well as the magnitude of its effects. A harmonic vibration is manifested in a Mössbauer spectrum as a broadening of the line profile and a decreasing of the line depth. For high amplitude vibrations the Mössbauer-spectral-absorption lines take a double peak profile. In Fig. 5d the Mössbauer spectrum of the vibrating stainless-steel foil for each one of the voltage amplitudes is shown (the spectra were obtained by time averaging each transmission surface). Note that the magnitude of the vibration effects on the spectra are higher than the quick line-motion effects on the transmission surface. Take, for instance, the lowest V_0 case from Fig. 5. The spectrum shows a well resolved two peak profile; with a 5 % relative transmission (without vibration 40 % relative transmission was recorded—see Fig. 2). Whereas the absorption line observed in the surface graph is evidently narrower and deeper, as can be directly checked in the phase trace curve shown in Fig. 5c, in which a 30 % effect is evidencing. The point is that what is spurious for the spectrum analysis (the whole vibration) is not for the self vibration characterization. Instead, the quick line-motion effect is an spurious effect for this characterization.

Finally, the fitted surface does not reproduce exactly the experimental transmission surface. By raw inspection of the transmission surfaces is evident that the absorption line does not behave like a rigid Lorentzian profile moving sinusoidally, as the fitting model propose. Conversely, the absorption line is thinner and deeper when it pass through the rest points than when it reaches the equilibrium points (maximum velocities). On other words, the absorption line spread and shrink periodically as it passes by these points. This behavior is more important as V_0 increases being negligible at low amplitudes (as in the used in Section 3). The proposed fitting model

does not cover this phase dependence behavior, therefore the depth and width fitting parameters should fall in the middle of the experimental extreme values. The spread of the absorption at high velocities might be originated on a dispersion of the PD velocity amplitudes or a chaotic noise over the PD movement. The quality of the experimental data allows a study of this features. However the proposed model allows a good determination of amplitude and phase-shift of the average sinusoidal movement, which was what we were looking for.

5 Discussion

The use of multiple velocities in synchronous Mössbauer acquisition increase considerably the experiment efficiency. Although, at low amplitude (see Section 3) a unique velocity position was enough to retrieve information of the oscillatory response. The use of more velocities is well justified due to the non-linearity of the velocity-transmission transfer curve given by the absorption line shape. In that sense, when the transmission rate response at a given velocity loses the pure harmonic behavior, the signal at different velocities allows to discern if the non linearities become from the absorption line shape or are originated in the voltage-velocity characteristic curve of the system under study. The choice of two velocities at both flanks of the absorption line improves considerably the characterization of low amplitude oscillations. Besides, a third velocity position at high energies allows a good quantification at a background energy, which is important to ensure a good estimation on the relative to background transmission rate at each velocity, which helps to dismiss spurious fluctuations or frequency dependent factors in the acquisition dead time.

In summary the use of multiple velocities allows to extend the maximum velocity limit previously indicated as 1 mm/s. In this work we proved that almost a maximum amplitude of 20.6 mm/s is attainable. Even more relevant is that this limit is not more determined by the velocity range of the sensitive absorption region of the absorption-line, but by ability to perform mechanics constant velocities movements. Instead of being an intrinsic limitation is a technical one.

Other interesting feature related to uniformly dispersed sampling velocities, is removal of nonlinearity, which was intrinsically presented in data interpretation. Indeed, single velocity data interpretation is restricted to the velocity-transmission transfer function (i.e the absorption line profile). However, the multiple velocity experiment allows to generate the surface graphs, in which a direct observation of the line velocity-position as a function of time (phase) is possible, even without considering the absorption line profile. The path that follows the absorption line in the velocity-time space is directly observed from these graphs.

Although amplitude and phase shift can be estimated from those surface graphs, a least square fit was used to quantify these values from the data. This procedure assures more precise values of those parameters. However, from the fit procedure not only the oscillatory movement is characterized, but also intrinsic parameters of the absorption line, i.e. the isomer shift, linewidth and depth. Therefore the proposed methodology serves as a tool to deconvolute those spectral parameters from unwanted vibrations. For this purpose the MCS must be triggered by the perturbation signal. However this practical application will be developed and discussed in a further work.

6 Conclusions

Vibration measurements using Mössbauer Effect Spectrometry was revisited. The technique capability is demonstrated by characterizing frequency and amplitude response of a commercial piezoelectric diaphragm using the constant-velocity mode. The smallest measured velocity-amplitude was 1.52 μm/s while the highest was 20.6 mm/s. In the position domain the highest position-amplitude was 1.3 μm at 2.4 kHz while the smallest amplitude was 0.7 nm at 4.5 kHz.

Acknowledgement We appreciate financial support to ANPCyT, Argentina (PICT 2785-2010).

References

1. Gilad, P., et al.: Application of the Mössbauer method to ear vibrations. J. Acoust. Soc. Am. **41**, 1232–1236 (1967)
2. Brafman, H., et al.: Use of the Mössbauer effect to measure small vibrations. Nucl. Intrum. Methods. **53**, 13–21 (1967)
3. Robles, L., et al.: Transient response of the basilar membrane measured in squirrel monkey using the Mössbauer effect. J. Acoust. Soc. Am. **59**, 926–939 (1976)
4. Lynch, T., et al.: Input impedance of the cochlea in cat. J. Acoust. Soc. Am. **72**, 108 (1982)
5. Robles, L., et al.: Basilar membrane mechanics at the base of the chinchilla cochlea. J. Acoust. Soc. Am. **80**, 1364–1374 (1986)
6. Ruggero, M.A., et al.: Middle-ear response in the chinchilla and its relationship to mechanics at the base of the cochlea. J. Acoust. Soc. Am. **87**, 1612–1629 (1990)
7. Ruggero, M.A., Rich, N.C.: Application of a commercially-manufactured Doppler-shift laser velocimeter to the measurement of basilar-membrane vibration. Hear. Res. **51**, 215–230 (1991)
8. Pasquevich, G.A., et al.: Local magnetic susceptibility by Mössbauer effect. In: CONFERENCIA Latinoamericana Sobre las Aplicaciones del Efecto Mössbauer (12 : 2010 : Lima), pp. 51–52. Abstracts book. Lima: LACAME, UNI, Fondo Editorial, UNMSM, Ediciones del Vicerrectorado Académico (2010)
9. Pasquevich, G.A., et al.: Determination of the iron atomic magnetic moments dynamics in the nanocrystalline ribbons Fe90Zr7B3 by Mössbauer magnetic scans. Phys., B Condens. Matter **384**, 348–350 (2006)
10. Veiga, A., et al.: Smooth driving of Mössbauer electromechanical transducers. Hyperfine Interact. **202**, 107–115 (2011)
11. Veiga, A., et al.: Advances in constant-velocity Mössbauer instrumentation. Hyperfine Interact. **167**, 905 (2006)